Effect of the insulator-metal transition on the phonon anomalies in La_2CuO_4

Claus Falter and Georg A. Hoffmann
Institut für Theoretische Physik II-Festkörperphysik, Universität Münster, Wilhelm-Klemm-Straße 10, D-48149 Münster, Germany
(Received 4 October 1999)

We investigate the experimentally observed anomalous softening of certain high-frequency oxygen bond-stretching modes during the insulator-metal transition via the underdoped phase in La_2CuO_4. The calculations show that the screening processes producing the softening behavior are well described in terms of charge fluctuations on the outer shells of the ions composing the crystal. In order to discriminate between the charge response in the insulator and the metal suitable models are used being consistent with rigorous sum rules for the density response in the long-wavelength limit of the various phases. In the case of the underdoped phase a response sum rule halfway between that of an insulator and a metal is proposed expressing a loss in the partial density of states for the Cu orbitals at the Fermi level.

I. INTRODUCTION

The question of the importance of the electron-phonon interaction (EPI) in the normal and superconducting states of the high-temperature superconductors (HTSC) is still under discussion, as well as its contribution to the mechanism of pairing in these materials. In particular, the specific feature of the layered cuprates, namely their strong nonlocal electronic charge response arising from a combination of weak screening and the ionic nature of the HTSC, leads to a large electron-phonon coupling.[1–4] These findings definitely add weight to the significance of the phonon contribution to the superconductivity in the cuprates.

The coupling between phonons and electrons generates a renormalization of the phonon frequencies, and if this is strong enough, characteristic phonon anomalies may occur in certain parts of the Brillouin zone for phonon branches where the coupling is allowed by symmetry. Perhaps the most interesting experimental evidence of a large and anomalous electron-phonon interaction, accompanied by corresponding phonon softening, is provided by inelastic neutron scattering in La_2CuO_4.[5–8] Here a strong softening of the high-frequency oxygen bond-stretching modes in the CuO plane is found when holes are doped into the insulating compound. The doping leads to a strong decrease of the oxygen breathing mode O_B^X [endpoint of the $\Sigma\sim(1,1,0)$ direction] and even more strongly for a second CuO bond-stretching mode at $\vec{q}=(0.5,0,0)$ called $\Delta_1/2$ in the following.

Recently, we have studied the softening of these phonons in the metallic, optimally doped phase of La_2CuO_4 and demonstrated that it is driven by long-range, nonlocal electron-phonon interaction effects of charge-fluctuation (CF) type.[9] Our investigations for the electronic charge redistribution which appears during this screening process in these modes have shown that dynamic charge ordering occurs in the form of localized charged stripes of alternating sign in the CuO plane, which is strongly interacting with the lattice vibrations under consideration. These phonon-induced stripes are stabilized by their mutual Coulomb interaction and such a screening process then leads to the strong decrease in frequency of the oxygen bond-stretching vibrations in the CuO plane.

In this paper we will discuss the experimentally observed softening of the O_B^X and the $\Delta_1/2$ mode as generated by the insulator-metal transition via the underdoped phase. The optimally doped metallic phase is described in the present paper following the approach of Ref. 9 within the framework of a local-density approximation (LDA) for the electronic band structure. For the calculations of the phonons in the underdoped phase and the insulating compound, where LDA cannot be applied because the latter always predicts a metallic state, we propose suitable models for the electronic density response based on certain sum rules for the electronic polarizability.

In Sec. II a short review of the theory and the modeling is given in order to provide a certain degree of self-consistency of the text. In Sec. III a way of modeling the density response of the underdoped and insulating phase of the HTSC is proposed. Furthermore, the calculated results for the phonon anomalies in La_2CuO_4 are presented and compared with the experiments. Subsequently, a summary is provided in Sec. IV.

II. REVIEW OF THE THEORY AND MODELING

In our theoretical description of the electronic density response and the electron-phonon interaction the local part is approximated by an *ab initio* rigid-ion model (RIM) taking into account ion softening as calculated from a tight-binding analysis of the electronic band structure. This results in effective ionic charges which are obtained from the orbital occupation numbers Q_μ of the μ (tight-binding) orbital in question, i.e.,

$$Q_\mu=\frac{2}{N}\sum_{n\vec{k}}|c_{\mu n}(\vec{k})|^2, \tag{1}$$

$c_{\mu n}(\vec{k})$ means the μ component of the eigenvector of band n at wave vector $\vec{k}$ from the first Brillouin zone; the summation in Eq. (1) runs over all occupied states. N denotes the numbers of elementary cells in the (periodic) crystal. For La_2CuO_4 our tight-binding analysis of the first-principles electronic band structure based on the LDA as given in Ref. 10 leads to the following electron configuration:[11] Cu $3d^{9.24}4s^{0.3}4p^{0.24}$; $O_{xy}2p^{5.42}$, $O_z2p^{5.47}$; La $5d^{0.72}$. The

corresponding effective ionic charges then are $Cu^{1.22+}$; $O_{xy}^{1.42-}$, $O_z^{1.47-}$; $La^{2.28+}$. In these calculations La $5d$, Cu $3d$, $4s$, $4p$, and O $2p$ states are included resulting altogether in a 31-band model (31 BM). The rigid-ion model with effective charges then serves, in general, as a reference system for the insulating phase of the HTSC. For a description of screening, particularly in the metallic phase of the HTSC, more or less localized electronic charge fluctuations (CF) on the outer shells of the ions are considered. This can be achieved by starting with the densities of the ions in the form

$$\rho_\alpha(r)=\rho_\alpha^0(r)+\sum_\lambda Q_\lambda \rho_\lambda^{\mathrm{CF}}(r). \tag{2}$$

$\rho_\alpha^0(r)$ is the density of the unperturbed ion assumed to be spherically symmetric and localized at the sublattice α of the crystal. The other contribution in Eq. (2) describes the CF in the electronic orbitals λ with amplitudes Q_λ and form factors (density distribution) $\rho_\lambda^{\mathrm{CF}}(r)$. The latter are approximated by a spherical average of the orbital densities of the outer ionic shells calculated in the LDA and taking self-interaction effects (SIC) into account according to Ref. 12.

Next, we investigate the total energy of the crystal, following Ref. 13, by assuming the density ρ of the crystal to be given as a superposition of overlapping densities of the ions. The latter are calculated within SIC-LDA. Experimental measurements of ρ in ionic crystals confirm such an approximation by overlapping ionic densities.[14] If we introduce additionally effective ionic charges, together with the Watson sphere approach,[15] such an approximation also holds in the HTSC.[3,11,16] Applying additionally the pair-potential approximation we obtain the following result for the total energy in our model:

$$E(R,\zeta)=\sum_{\vec{a}\alpha} E_{s\alpha}^{\vec{a}}(\zeta)+\frac{1}{2}{\sum_{\substack{\vec{a}\alpha\\ \vec{b}\beta}}}' \phi_{\alpha\beta}(\vec{R}_\beta^{\vec{b}}-\vec{R}_\alpha^{\vec{a}},\zeta). \tag{3}$$

The energy becomes a function of the configuration of the ions $\{R\}$ and the electronic degrees of freedom (EDF) $\{\zeta\}$ of the density, i.e., in our case here the CF $\{Q_\lambda\}$. $E_{s\alpha}^{\vec{a}}$ are the (self-) energies of the individual ions. $\vec{a},\vec{b}$ denote the elementary cells in the crystal and α,β the sublattices ($\vec{R}_\alpha^{\vec{a}}=\vec{R}^{\vec{a}}+\vec{R}^{\alpha}$). The second term in Eq. (3) gives the interaction energy of the system expressed by the pair interactions $\phi_{\alpha\beta}$. The prime in Eq. (3) means that the self-term has to be left out of the summation. $E_{s\alpha}^{\vec{a}}$ as well as $\phi_{\alpha\beta}$ in general depend upon ζ via ρ_α.

For a given ion configuration $\{R\}$ the electronic degrees of freedom $\{\zeta\}$ adjust themselves according to the minimum principle for the energy, i.e.,

$$\frac{\partial E(R,\zeta)}{\partial \zeta}=0. \tag{4}$$

Using Eq. (4) we can derive an expression for the atomic force constants, and accordingly, the dynamical matrix in harmonic approximation

$$t_{ij}^{\alpha\beta}(\vec{q})=[t_{ij}^{\alpha\beta}(\vec{q})]_{\mathrm{RIM}}-\frac{1}{\sqrt{M_\alpha M_\beta}} \times\sum_{\kappa,\kappa'}[B_i^{\kappa\alpha}(\vec{q})]^*[C^{-1}(\vec{q})]_{\kappa\kappa'}[B_j^{\kappa'\beta}(\vec{q})]. \tag{5}$$

$t_{ij}^{\alpha\beta}(\vec{q})$ are the elements of the dynamical matrix at wave vector $\vec{q}$ from the first Brillouin zone, $[t_{ij}^{\alpha\beta}(\vec{q})]_{\mathrm{RIM}}$ gives the contribution of the RIM, M_α and M_β represent the masses of the ions, and the quantities $B(\vec{q})$ and $C(\vec{q})$ describe the Fourier transforms of the coupling coefficients

$$\vec{B}_{\kappa\,\beta}^{\vec{a}\,\vec{b}}=\frac{\partial^2 E(R,\zeta)}{\partial\zeta_\kappa^{\vec{a}}\partial\vec{R}_\beta^{\vec{b}}} \tag{6}$$

and

$$C_{\kappa\,\kappa'}^{\vec{a}\,\vec{b}}=\frac{\partial^2 E(R,\zeta)}{\partial\zeta_\kappa^{\vec{a}}\partial\zeta_{\kappa'}^{\vec{b}}}. \tag{7}$$

The derivatives in Eqs. (6) and (7) have to be performed at the equilibrium positions. κ describes the electronic degree of freedom in an elementary cell of the crystal. The B coefficients give the interaction (coupling) between the EDF and the ions and the C coefficients between the EDF, i.e., between the charge fluctuations in our case here. Equations (4)–(7) are generally valid for arbitrary EDF, and, in particular, are independent of our specific model for the density in Eq. (2) and of the approximation (3) for the energy of the crystal.

The matrix $C_{\kappa\kappa'}(\vec{q})$ of the EDF-EDF interaction can also be decomposed according to Ref. 3 as

$$C=\Pi^{-1}+\tilde{V}. \tag{8}$$

Π^{-1} contains the kinetic one-particle part to the interaction and $\tilde{V}$ the Hartree and exchange-correlation contribution. The quantity needed for the dynamical matrix in Eq. (5) is C^{-1} which can be written as

$$C^{-1}=\Pi(1+\tilde{V}\Pi)^{-1}\equiv\Pi\varepsilon^{-1}. \tag{9}$$

C^{-1} is closely related to the density response function (matrix) and to the inverse dielectric function (matrix) ε^{-1}, respectively.[3] It can be calculated approximatively from a tight-binding model of the electronic band structure where the electronic polarizability Π is given as

$$\Pi_{\kappa\kappa'}(\vec{q})=-\frac{2}{N}\sum_{\substack{n,n'\\ \vec{k}}}\frac{f_{n'}(\vec{k}+\vec{q})-f_n(\vec{k})}{E_{n'}(\vec{k}+\vec{q})-E_n(\vec{k})} \times[C_{\kappa n}^*(\vec{k})C_{\kappa n'}(\vec{k}+\vec{q})][C_{\kappa' n}^*(\vec{k})C_{\kappa' n'}(\vec{k}+\vec{q})]^*. \tag{10}$$

f, E, and C are the occupation numbers, the electronic band structure, and the expansion coefficients of the Bloch functions in terms of the tight-binding functions.

In our discussion of the phonon anomalies for the optimally doped, metallic phase of La_2CuO_4 in Ref. 9 we have allowed for La $5d$, Cu $3d$, $4s$, $4p$, and O $2p$ charge fluc-

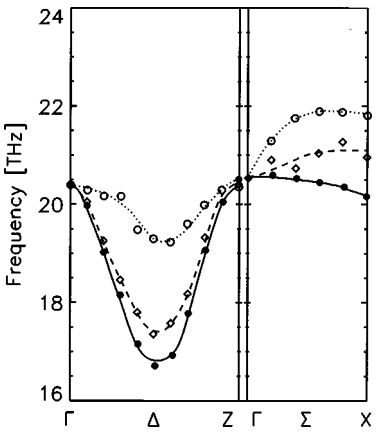

FIG. 1. Experimental results for the highest Δ_1 and Σ_1 branches for $La_{2-x}Sr_xCuO_4$ according to Refs. 5 and 8. The open circles represent the insulating phase ($x=0$), the full circles the optimally doped metallic phase ($x=0.15$), and the diamonds the underdoped phase ($x=0.1$). The lines are a guide to the eye.

tuations. Consistent with these EDF we have calculated the electronic polarizability Π in the tight-binding representation from Eq. (10) using the 31 BM for the electronic band structure. The form factors ρ_λ are approximated by the spherically averaged orbital density of the La $5d$, Cu $3d$, $4s$, $4p$, and O $2p$ shell. For more calculational details to obtain the coupling coefficients $\vec{B}$ and C we refer to our earlier work; see, e.g., Refs. 3 and 17.

III. MODELING OF THE DENSITY RESPONSE AND RESULTS FOR THE ANOMALOUS PHONON SOFTENING

In this section we discuss the experimentally observed softening of the planar oxygen breathing mode O_B^X at the X point of the Brillouin zone, and of the $\Delta_1/2$ mode as generated by the insulator-metal transition. As can be extracted from the experimental results[5,6,8] displayed in Fig. 1, there is an increase in the degree of softening for the corresponding Δ_1 and Σ_1 branch when going from the insulating phase (open circles) to the optimally doped metallic phase (full circles), passing through the underdoped phase (diamonds). The displacement patterns of the two high-frequency oxygen bond-stretching modes $\Delta_1/2$ and O_B^X are shown in Fig. 2.

In Ref. 9 we have demonstrated that the experimental dispersion curves for the optimally doped $La_{1.85}Sr_{0.15}CuO_4$ probe (full curves in Fig. 1) are well described by our calculations within the 31 BM for the electronic band structure. The strong softening for $\Delta_1/2$ and the downward dispersion of the Σ_1 branch found in the experiments has been attributed in these calculations to the growing importance of the more extended orbitals ($4s$, $4p$ in our model) at the Cu ion to the charge response.

In this paper we propose a simple model for the polarizability matrix Π in Eq. (10) to describe the metallic, optimally doped phase of La_2CuO_4. Its form is suggested by our (LDA based) results for Π in the 31 BM. These investigations indicate that in the metallic phase the diagonal of Π dominates by far. Hence, we approximate Π by a diagonal matrix. Assuming such a model we obtain results for the phonon dispersion which are in nice agreement with those as obtained with the complete Π matrix of the 31 BM in Ref. 9. Only the matrix elements for the Cu $4s$ and Cu $4p$ orbitals have to be readjusted in order to optimize the agreement with the full calculation, while all the other diagonal elements can be taken over from the calculated polarizability matrix. The full curve in Fig. 3 represents the calculations for the anomalous phonon dispersion with such a model for the metallic phase. Comparing with the experiments in Fig. 1 we find a good agreement of the calculated and the measured dispersion curves.

In order to discriminate in our approach between a metallic and an insulating density response behavior (the latter cannot be obtained within the LDA) we use the long-wavelength limit of the electronic polarizability Π, as given in Ref. 3. In the metallic phase the partial density of states

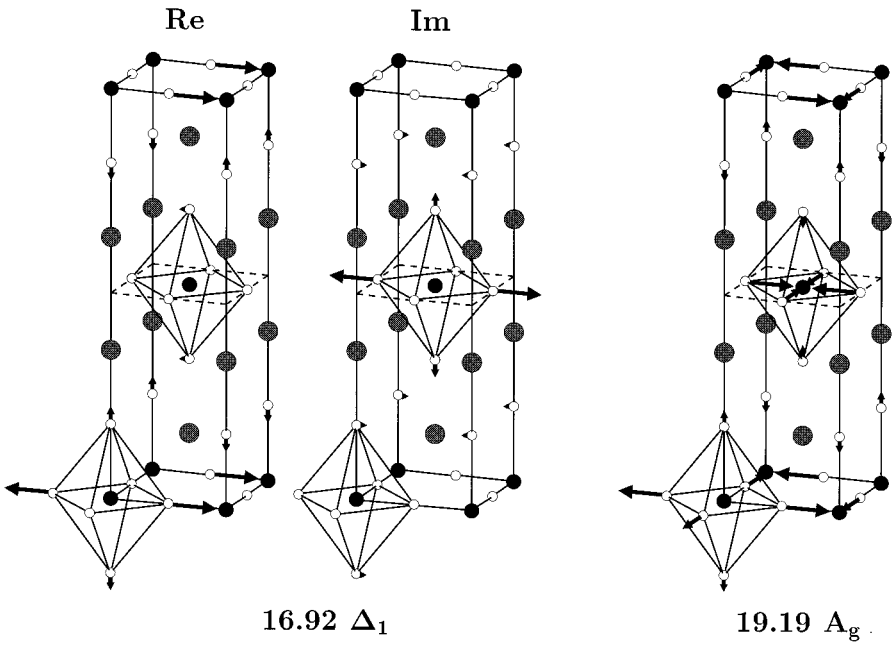

FIG. 2. Displacement pattern of the two high-frequency oxygen bond-stretching vibrations O_B^X (19.19 THz) and $\Delta_1/2$ (16.92 THz) as calculated from the diagonal approximation of the complete polarizability matrix for metallic La_2CuO_4; compare with the text. From the left to the right in the figure the real part of $\Delta_1/2$, the imaginary part of $\Delta_1/2$ and O_B^X is shown.

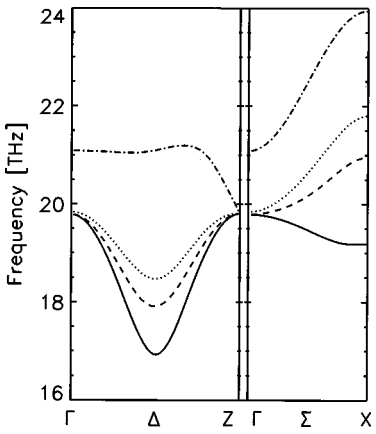

FIG. 3. Calculated result for the phonon branches shown in Fig. 1 using the models proposed in the text for the electronic density response in the various phases. The dotted curves give the results for the insulating phase, the broken curves for the underdoped phase, and the full curves for the metallic phase. For comparison the results for the rigid-ion model without any charge fluctuations (reference model for the insulating phase in the HTSC) are also displayed (dash-dotted curves).

(PDOS) at the Fermi level $Z_\kappa(\varepsilon_F)$ is related to the polarizability matrix at zero wave vector according to

$$\sum_{\kappa'} \Pi_{\kappa\kappa'}(\vec{0}) = Z_\kappa(\varepsilon_F), \tag{11}$$

and the total density of states is defined as

$$Z(\varepsilon) = \sum_{\kappa} Z_\kappa(\varepsilon). \tag{12}$$

Noting that the density of states at the Fermi level vanishes in an insulator, we see that Eq. (11) applies when equating $Z_\kappa(\varepsilon_F)$ formally to zero on the right-hand side. More precisely we get for an insulator[3]

$$\sum_{\kappa'} \Pi_{\kappa\kappa'}(\vec{q}) = O(q) \tag{13}$$

and

$$\sum_{\kappa,\kappa'} \Pi_{\kappa\kappa'}(\vec{q}) = O(q^2) \tag{14}$$

as $\vec{q} \to \vec{0}$. This means that there are necessarily some couplings $\Pi^{\vec{a}\,\vec{b}}_{\kappa\,\kappa'}$ of different charge fluctuations, $\vec{a}\kappa \neq \vec{b}\kappa'$, for an insulator in the expression for $\Pi_{\kappa\kappa'}(\vec{q})$ according to Eq. (15),

$$\Pi_{\kappa\kappa'}(\vec{q}) = \sum_{\vec{b}} \Pi^{\vec{0}\,\vec{b}}_{\kappa\,\kappa'} e^{i\vec{q}(\vec{R}_{\kappa'} - \vec{R}_\kappa)}. \tag{15}$$

For the description of the underdoped phase of the HTSC we propose a model with response properties in between those of a metal and an insulator. We call this the pseudogap model (PGM) and define this model by the following long-wavelength response behavior:

$$\sum_{\kappa'} \Pi_{\kappa\kappa'}(\vec{q} \to \vec{0}) = \begin{cases} O(q) & \text{for Cu orbitals} \\ Z_\kappa(\varepsilon_F) & \text{otherwise.} \end{cases} \tag{16}$$

Adopting Eq. (16) for the electronic polarizability we regard the pseudogap as a loss in the density of states in the CuO plane at the Fermi level, and we simulate this fact by assuming that the PDOS for Cu states vanishes at ε_F. Simultaneously, the Cu polarizability will be reduced. This seems to be a reasonable assumption because the self-interaction will shift the strongly localized occupied Cu $3d$ states below the O $2p$ states and the La $5d$ states in the insulating phase.[18]

In our model for the pseudogap insulator and the insulator, respectively, only $3d$ orbitals are considered at the Cu ion. Such an assumption is consistent (at least for the insulating phase) with the SIC-LSD calculations for the projected density of states as reported in Ref. 18. Furthermore, the nearest-neighbor approximation in Eq. (15) is adopted concerning the coupling coefficients. As a consequence of the polarizability sum rules given in Eqs. (13) and (16) the coupling of different CF have to be taken into account. The notation Π(Cu), Π(Cu-O), etc., is used in the following as a shorthand notation for the coupling coefficients $\Pi^{\vec{a}\,\vec{a}}_{\kappa\,\kappa'}$, $\Pi^{\vec{a}\,\vec{b}}_{\kappa\,\kappa'}$, $(\vec{a}\kappa \neq \vec{b}\kappa')$ in our models (units are in eV^{-1}).

In the calculations for the PGM the sum rule in Eq. (16) must be fulfilled. In order to satisfy this requirement we have made the following choice of the coupling coefficients. This obviously is not unique, but it should reflect qualitatively the correct physics. From the above discussion the polarizability Π(Cu) should be reduced as compared with the metallic case. We assume a reduction by a factor of about 3 compared to the metal. Thus we end up with $\Pi(\mathrm{Cu}) = 1$ for the PGM. Moreover, the PDOS for Cu at the Fermi level, as obtained in the 31 BM, is redistributed among $\mathrm{O}_{x,y,z}$. Further, we assume that Π(Cu-O) is much larger than Π(Cu-La) and we assume the ratio of both to 4 in order to reduce the number of free parameters in the model. Using Eq. (16) and taking over the calculated results of $Z_\kappa(\varepsilon_F)$ for $\mathrm{O}_{x,y,z}$ and La from the 31 BM, we finally obtain for the PGM

$$\Pi(\mathrm{Cu}) = 1,\ \Pi(\mathrm{O}_{xy}) = 1.25,\ \Pi(\mathrm{O}_z) = 0.855,\ \Pi(\mathrm{La}) = 0.185,$$

$$\Pi(\mathrm{Cu\text{-}O}_{xyz}) = -0.125,\ \Pi(\mathrm{Cu\text{-}La}) = -0.031\,25,$$

while all other couplings in the elementary cell have been neglected.

In the model for the insulator (IM) the polarizability for the Cu is still further reduced to the value $\Pi(\mathrm{Cu}) = 0.1$. The other self-coupling, i.e., for O_{xy}, O_z, and La are calculated as in the PGM but take the smaller Cu polarizability into account. Ignoring Π(La-La) and $\Pi(\mathrm{O}_z\text{-}\mathrm{O}_z)$ and keeping the ratio of Π(Cu-O) and Π(Cu-La) fixed as in the PGM, we finally get the following couplings fulfilling the sum rules from Eq. (13) for the insulator:

$$\Pi(\mathrm{Cu}) = 0.1,\ \Pi(\mathrm{O}_{xy}) = 1.025,\ \Pi(\mathrm{O}_z) = 0.7425,$$

$$\Pi(\mathrm{La}) = 0.0725,\ \Pi(\mathrm{Cu\text{-}O}_{xyz}) = -0.0125,$$

$$\Pi(\mathrm{Cu\text{-}La}) = -0.003\,125,\ \Pi(\mathrm{O}_x\text{-}\mathrm{O}_y) = -0.0825,$$

$$\Pi(\mathrm{O}_{xy}\text{-}\mathrm{O}_z) = -0.1675,\ \Pi(\mathrm{O}_z\text{-La}) = -0.06.$$

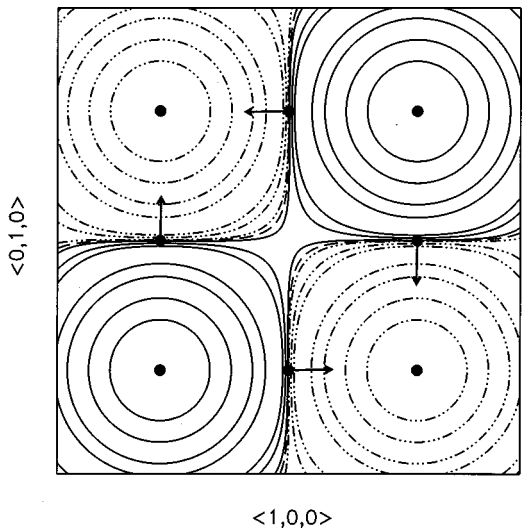

FIG. 4. Contourplot of the phonon-induced charge-density redistribution $\delta\rho$ (scaled by a factor 10^4) for O_B^X resulting from the charge fluctuations in the metallic phase of La_2CuO_4. The contourlines are plotted for the levels 0, ± 0.01, ± 0.05, ± 0.1, ± 0.5, ± 1.0, ± 2.5, ± 5.0, in decreasing order when moving from the center of the ions to the outside. $\delta\rho$ has been calculated applying the diagonal approximation of the complete polarizability matrix. The moving O_x, O_y ions are represented as dots. The full lines represent the regions where the electrons are accumulated. Units are in electrons/a_B^3.

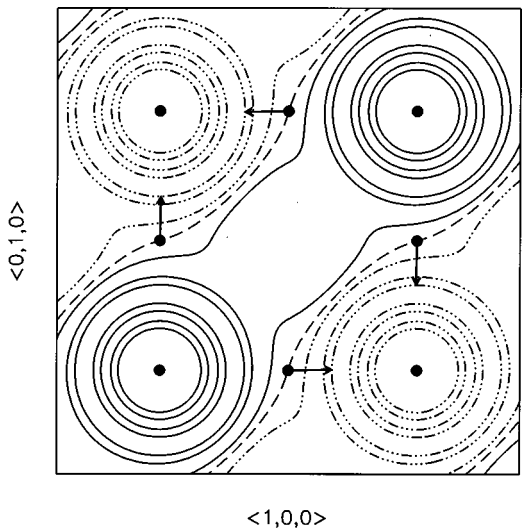

FIG. 5. Same as in Fig. 4 but for the insulating phase of La_2CuO_4. The corresponding model for the insulator as explained in the text has been used to calculate the charge response.

It is interesting to compare the important copper and oxygen self-couplings for the metal [$\Pi(\text{Cu } d)=2.8$, $\Pi(O_{xy})=0.2$, $\Pi(O_z)=0.13$, $\Pi(\text{La})=0.06$, $\Pi(\text{Cu } s)=0.05$, $\Pi(\text{Cu } p)=0.01$] with the above choices for the pseudogap insulator and the insulator, respectively. While the polarizability for Cu decreases according to our assumption, which was guided by the fact that the occupied Cu d states are pushed below the O p states, the polarizability increases for O_{xy} and O_z in the PGM and IM. This can be qualitatively understood if the top of the valence bands in these phases is dominated by states of O_{xy} and O_z character. This conjecture is supported for insulating La_2CuO_4 by the electronic structure calculations of Ref. 18 within the self-interaction corrected density-functional formalism.

The calculations for the anomalous phonon dispersion with the pseudogap and the insulator model, respectively, are shown in Fig. 3, together with the calculated data for the metallic phase. For comparison, the results of the RIM are also displayed in the figure (dash-dotted curves). The dotted curves are for the IM, the broken curves for the PGM, and the full curves for the metallic phase. Comparing these results with the corresponding experimental data from Fig. 1 we generally find good agreement. In particular, the increase in softening for $\Delta_1/2$ and O_B^X induced by the insulator-metal transition via the underdoped phase is correctly described by our modeling of the electronic density response.

Figures 4 and 5 display the calculated results of the phonon-induced charge-density redistribution resulting from the CF for the O_B^X mode in the metallic and insulating phase. For the metallic phase the simple diagonal model for Π has been used. As mentioned in the Introduction, the alternating charged stripes along the diagonals in the CuO plane are clearly visible. Comparing both calculations with each other the charge response displays a distinctively higher degree of localization in the insulating phase than in the metal.

IV. SUMMARY

In this paper we have presented a study of the experimentally observed anomalous phonon softening in La_2CuO_4 during the transition from the insulating to the metallic phase via the underdoped regime. The pronounced phonon renormalization seen in the experiments documents the importance of the coupling of electrons and phonons in La_2CuO_4. In order to deal with the problem theoretically, different models for the charge response in the various phases have been proposed. The metallic phase is described by a simple diagonal approximation of the complete polarizability matrix, as obtained by using a realistic electronic band structure (31 BM) for La_2CuO_4. The density response simulating the underdoped and insulating phase has been modeled by fulfilling the requirements of the long-wavelength sum rules for the electronic polarizability. An important aspect in these model descriptions, which leads to good agreement with the experimental results for the phonon dispersion, is the assumed depletion of the localized Cu $3d$ states at the Fermi level and the simultaneous reduction of the polarizability at the Cu ion. Finally, the calculation of the phonon-induced charge response shows that dynamic charge ordering appears in the CuO plane in the form of localized stripes interacting strongly with the lattice vibrations. The degree of localization of this phonon-induced charge redistribution is increased in the insulating phase as compared with the metal. Such a strong coupling, which is considerably enhanced in the optimally doped metallic probe, definitely adds weight to the significance of phonon contribution to the superconductivity in the cuprates.

ACKNOWLEDGMENT

We greatly appreciate the financial support by the Deutsche Forschungsgemeinschaft.

[1] H. Krakauer, W. E. Pickett, and R. E. Cohen, Phys. Rev. B **47**, 1002 (1993).
[2] C. Falter, M. Klenner, and W. Ludwig, Phys. Lett. A **165**, 260 (1992).
[3] C. Falter, M. Klenner, and W. Ludwig, Phys. Rev. B **47**, 5390 (1993).
[4] C. Falter, M. Klenner, and G. A. Hoffmann, Phys. Rev. B **57**, 14 444 (1998).
[5] L. Pintschovius and W. Reichardt, in *Physical Properties of High Temperature Superconductors IV*, edited by D. M. Ginsberg (World Scientific, Singapore, 1994), pp. 295–374.
[6] L. Pintschovius and M. Braden, J. Low Temp. Phys. **105**, 812 (1996).
[7] R. J. Mc Queeney, Y. Petrov, T. Egami, M. Yethiray, G. Shirane, and Y. Endoh, Phys. Rev. Lett. **82**, 628 (1999).
[8] L. Pintschovius and M. Braden, Phys. Rev. B **60**, 15 039 (1999).
[9] C. Falter, M. Klenner, G. A. Hoffmann, and Q. Chen, Phys. Rev. B **55**, 3308 (1997).
[10] M. J. De Weert, D. A. Papaconstantopoulos, and W. E. Pickett, Phys. Rev. B **39**, 4235 (1989).
[11] C. Falter, M. Klenner, and G. A. Hoffmann, Phys. Rev. B **52**, 3702 (1995).
[12] J. P. Perdew and A. Zunger, Phys. Rev. B **23**, 5048 (1981).
[13] R. G. Gordon and Y. S. Kim, J. Chem. Phys. **56**, 3122 (1972).
[14] O. V. Ivanov and E. G. Maksimov, Zh. Eksp. Teor. Fiz. **108**, 1841 (1995) [JETP **81**, 1008 (1995)].
[15] R. E. Watson, Phys. Rev. **111**, 1108 (1958).
[16] H. Krakauer, W. E. Pickett, and R. E. Cohen, J. Supercond. **1**, 111 (1988).
[17] C. Falter, M. Klenner, G. A. Hoffmann, and F. Schnetgöke, Phys. Rev. B **60**, 12 051 (1999).
[18] A. Svane, Phys. Rev. Lett. **68**, 1900 (1992).